Suppression of experimental autoimmune encephalomyelitis by extracellular adherence protein of *Staphylococcus aureus*

Changping Xie,[2] Pilar Alcaide,[4] Brian V. Geisbrecht,[3] Darius Schneider,[2] Mathias Herrmann,[5] Klaus T. Preissner,[6] Francis W. Luscinskas,[4] and Triantafyllos Chavakis[1]

[1]Experimental Immunology Branch, National Cancer Institute, National Institutes of Health, Bethesda, MD 20892
[2]Department of Internal Medicine I, University Heidelberg, D-69120 Heidelberg, Germany
[3]Division of Cell Biology and Biophysics, School of Biological Sciences, University of Missouri-Kansas City, Kansas City, MO 64110
[4]Department of Pathology, Brigham and Women's Hospital, Harvard Medical School, Boston, MA 02115
[5]Institute of Medical Microbiology and Hygiene, University of Saarland Hospital, D-66421 Homburg/Saar, Germany
[6]Institute for Biochemistry, Medical School, Justus-Liebig-University, D-35392 Giessen, Germany

Multiple sclerosis (MS) is a devastating inflammatory disorder of the central nervous system (CNS). A major hallmark of MS is the infiltration of T cells reactive against myelin components. T cell infiltration is mediated by the interaction of integrins of the β1 and β2 family expressed by lymphocytes with their endothelial counter-receptors, vascular cell adhesion molecule 1 and intercellular adhesion molecule (ICAM)-1, respectively. We have reported previously that extracellular adherence protein (Eap) of *Staphylococcus aureus* exerts anti-inflammatory activities by interacting with ICAM-1 and blocking β2-integrin–dependent neutrophil recruitment. Here, we report that Eap inhibits experimental autoimmune encephalomyelitis (EAE) in mice. In vitro, Eap reduced adhesion of peripheral blood T cells to immobilized ICAM-1 as well as their adhesion and transmigration of TNF-activated human endothelium under static and shear flow conditions. These inhibitory effects were corroborated in two mouse models of inflammation. In a delayed-type hypersensitivity model, both T cell infiltration and the corresponding tissue edema were significantly reduced by Eap. In addition, Eap administration prevented the development of EAE and markedly decreased infiltration of inflammatory cells into the CNS. Strikingly, intervention with Eap after the onset of EAE suppressed the disease. Collectively, our findings indicate that Eap represents an attractive treatment for autoimmune neuroinflammatory disorders such as MS.

CORRESPONDENCE
Triantafyllos Chavakis:
chavakist@mail.nih.gov

Abbreviations used: BBB, blood–brain barrier; CNS, central nervous system; DTH, delayed-type hypersensitivity; EAE, experimental autoimmune encephalomyelitis; Eap, extracellular adherence protein; HUVEC, human umbilical vein endothelial cell; ICAM, intercellular adhesion molecule; MOG, myelin oligodendrocyte glycoprotein; MS, multiple sclerosis; PBT, peripheral blood T; VCAM, vascular cell adhesion molecule.

Multiple sclerosis (MS) and its animal model, experimental autoimmune encephalomyelitis (EAE), are demyelinating diseases of the central nervous system (CNS) mediated by autoreactive T cells that penetrate through the blood–brain barrier (BBB) into the brain parenchyma. These T cells initiate autoimmune responses against antigens in the myelin sheath of the CNS, including myelin basic protein or myelin oligodendrocyte protein (1). Thus, the recruitment of autoreactive lymphocytes represents a crucial pathogenetic event in initiating CNS inflammation, and interfering with the homing of these cells may represent a feasible therapeutic approach for both EAE and MS.

Lymphocyte extravasation requires a well-coordinated sequence of adhesive and signaling events, including selectin-mediated rolling, chemoattractant-induced integrin activation, integrin-dependent firm adhesion, and the subsequent transendothelial migration (2). During adhesion and transmigration, integrins of the β1 and β2 family, such as VLA-4 (α4β1) or LFA-1 (αLβ2), bind to their endothelial counter-receptors vascular cell adhesion molecule (VCAM)-1 and intercellular adhesion molecule (ICAM)-1, respectively. Numerous studies have shown that adhesion of lymphocytes to inflamed brain vessels during EAE is mainly mediated by the VLA-4–VCAM-1 system (3, 4), although there is also evidence pointing to the role of the LFA-1–ICAM-1 interaction (5, 6). Recent studies indicated that both systems may have a distinct contribution in the

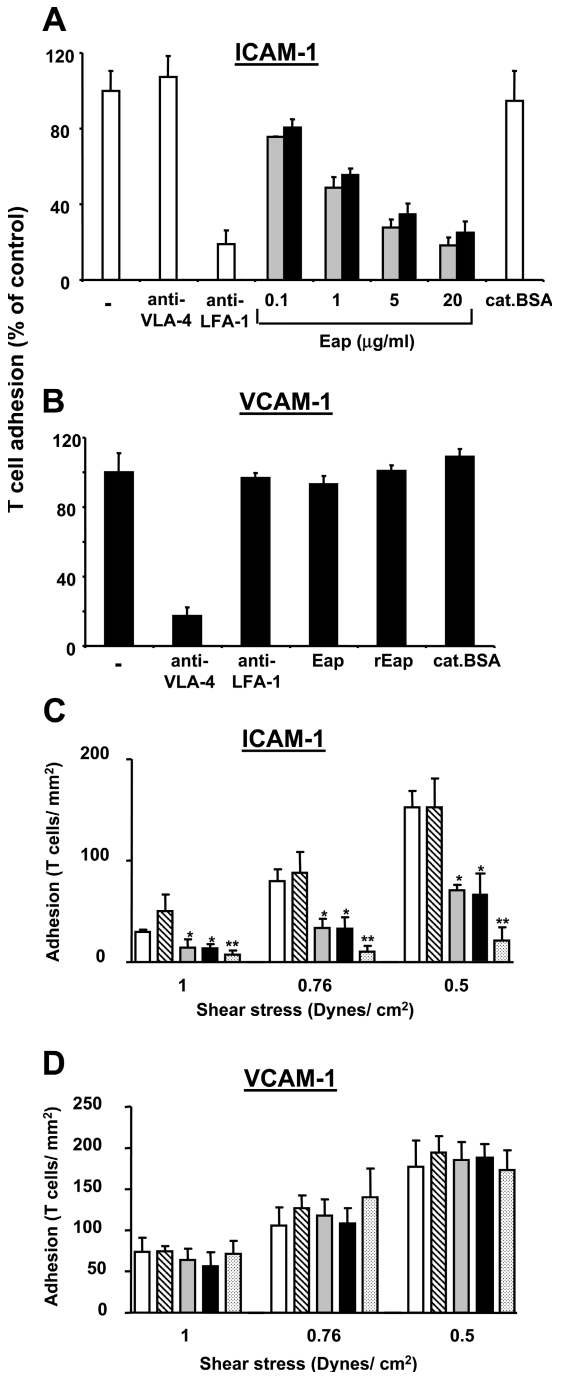

Figure 1. Eap inhibits T cell adhesion to ICAM-1. (A) The adhesion of T cells to immobilized ICAM-1 is shown in the absence (white bars) or presence of blocking mAb against VLA-4, mAb against LFA-1 (each at 20 μg/ml), increasing concentrations of purified (gray bars), or recombinant (black bars) Eap, or cationic BSA (20 μg/ml). (B) The adhesion of T cells to immobilized VCAM-1 is shown in the absence or presence of blocking mAb against VLA-4, mAb against LFA-1 (each at 20 μg/ml), purified Eap, recombinant Eap, or cationic BSA (each at 20 μg/ml). Cell adhesion is expressed relative to control (in the absence of competitor). Data are mean ± SD ($n = 3$) of a typical experiment; similar results were obtained in three separate experiments. (C and D) Adhesion of T cells to immobilized ICAM-1 (C) or VCAM-1 (D) under laminar shear flow conditions is shown in the absence (white bars) or presence of cationic BSA (diagonally striped bars), purified Eap (gray bars), recombinant Eap (black bars), or anti-LFA-1 mAb (dotted bars) (each at 20 μg/ml). Data are mean ± SEM, $n = 3$ separate experiments. *, $P < 0.05$. **, $P < 0.01$.

recruitment of encephalitogenic T cells. Although the VLA-4–VCAM-1 interaction predominantly mediates the initial adhesion to the inflamed vessels, LFA-1–ICAM-1 are engaged in the subsequent transendothelial migration of T cells (7, 8).

To date, therapeutic approaches targeting adhesion molecules have focused predominantly on the blockade of the VLA-4–VCAM-1 system (9). An antibody to VLA-4 that ameliorated EAE in mice was humanized (natalizumab) and demonstrated encouraging clinical efficacy for the treatment of patients with relapsing forms of multiple sclerosis. However, a few cases of fatal progressive multifocal leukoencephalopathy attributed to natalizumab prompted its withdrawal (9). Thus, the need for other adhesion molecule–based therapies is emerging. In contrast with the VLA-4–VCAM-1 system, only a few studies have addressed the role of the LFA-1–ICAM-1 system as a target in EAE, although ICAM-1 is clearly up-regulated in EAE and MS, and serum levels of soluble ICAM-1 were found to be elevated in MS patients with clinically symptomatic disease (5, 6, 10).

Extracellular adherence protein (Eap), also designated MHC class II analogous protein (Map) or P70, is a secreted protein from *Staphylococcus aureus*. Eap has a very broad repertoire of binding interactions to host extracellular matrix components (11, 12). Recently, we demonstrated a mechanism used by *S. aureus* to escape the host immune system that was attributed to the very potent antiinflammatory function of Eap. In particular, we found Eap to undergo a direct interaction with ICAM-1 that resulted in the disruption of integrin-dependent neutrophil–endothelial interactions (13). Strikingly, Eap was even more potent than blocking antibodies against the β2-integrin receptors or against ICAM-1.

These observations prompted us to investigate whether Eap could be feasible to interfere with T cell–adhesive mechanisms in EAE. In the present study, we show that Eap inhibits the LFA-1–ICAM-1 interaction and the T cell–endothelial interactions in vitro and in vivo. Furthermore, administration of Eap not only prevented the development of EAE, but Eap treatment reverted the disease and repressed its progress after its onset. Thus, Eap may represent a promising new therapy for chronic inflammatory diseases such as EAE and MS.

RESULTS

Eap blocks adhesion of T cells to ICAM-1

We have previously shown that Eap interferes with the interaction between ICAM-1 and its β2-integrin counter-receptors Mac-1 and LFA-1, thereby blocking neutrophil recruitment (13). To test whether Eap might interfere with T cell recruitment, we first examined the adhesion of peripheral blood T (PBT) cells to immobilized ICAM-1 and VCAM-1.

As shown in Fig. 1, the adhesion of PBT cells to immobilized ICAM-1 was mediated by LFA-1, whereas adhesion to VCAM-1 was dependent on β1-integrins. Under both static (Fig. 1, A and B) and physiologic flow conditions (Fig. 1, C and D), both purified and recombinant Eap dose-dependently inhibited the adhesion of PBT cells to immobilized ICAM-1, whereas adhesion of PBT cells to VCAM-1 was not affected in the presence of Eap. The inhibitory effect of Eap on the adhesion of PBT cells to ICAM-1 was comparable to the effect of blocking mAb to LFA-1 (Fig. 1). As Eap is a cationic protein, we engaged cationic BSA as a negative control, which did not affect LFA-1– or VLA-4–dependent adhesion to ICAM-1 or VCAM-1, respectively (Fig. 1).

Interference of Eap with T cell–endothelial cell interactions under static and physiologic flow conditions

As Eap blocks the adhesion of PBT cells to ICAM-1, we further determined whether Eap interferes with PBT cell–endothelial cell interactions. Therefore, the adhesion of PBT cells to endothelial cells as well as the transmigration of PBT cells through endothelial cell monolayers was studied under static and physiologic flow conditions. Under static conditions, the adhesion of PBT cells to TNF-α–prestimulated endothelial cells was mainly dependent on VLA-4, whereas the LFA-1–ICAM-1 system mediates a smaller portion of the T cell adhesion to endothelial cells under these conditions (Fig. 2 A). Both purified and recombinant Eap partially blocked adhesion of PBT cells to endothelial cells; the maximal inhibition observed was ∼35–40% and was comparable to the inhibition obtained with blocking mAb to LFA-1 (Fig. 2 A). In contrast, transendothelial migration of PBT cells was predominantly mediated by the LFA-1–ICAM-1 interaction; in this case, both purified and recombinant Eap were more potent in blocking PBT cell transendothelial migration (Fig. 2 B). As a negative control, cationic BSA did not influence PBT cell adhesion or transmigration.

Because the PBT cell–endothelial cell interactions under physiologic flow conditions simulate in vivo physiological shear flow, we studied the effect of Eap under defined shear flow in vitro (14, 15). As previously reported, PBT cell adhesion to TNF-α–prestimulated endothelial cells under physiologic flow in vitro is mainly dependent on the VLA-4–VCAM-1 adhesion pathway and to a lesser extent on the LFA-1–ICAM-1 pathway, whereas transmigration was primarily LFA-1–ICAM-1 dependent (7, 14, 16). Consistent with these prior observations, here we show that purified or recombinant Eap (data with recombinant Eap not shown) as well as blocking mAb to LFA-1 had no statistically significant effect on adhesion of PBT cells to TNF-α–activated human umbilical vein endothelial cell (HUVEC) monolayers under flow conditions (Fig. 3 A), whereas transendothelial migration was significantly blocked by Eap or mAb to LFA-1 (Fig. 3 B). In contrast, no effect of cationic BSA was observed. Collectively, these data (Figs. 1–3) indicate that Eap interferes with the LFA-1–ICAM-1–dependent component of T cell–endothelial interaction pathway under both static and physiologic flow conditions in vitro. This inhibitory effect of Eap is specific and cannot be attributed to a nonspecific effect of the cationic charge of Eap.

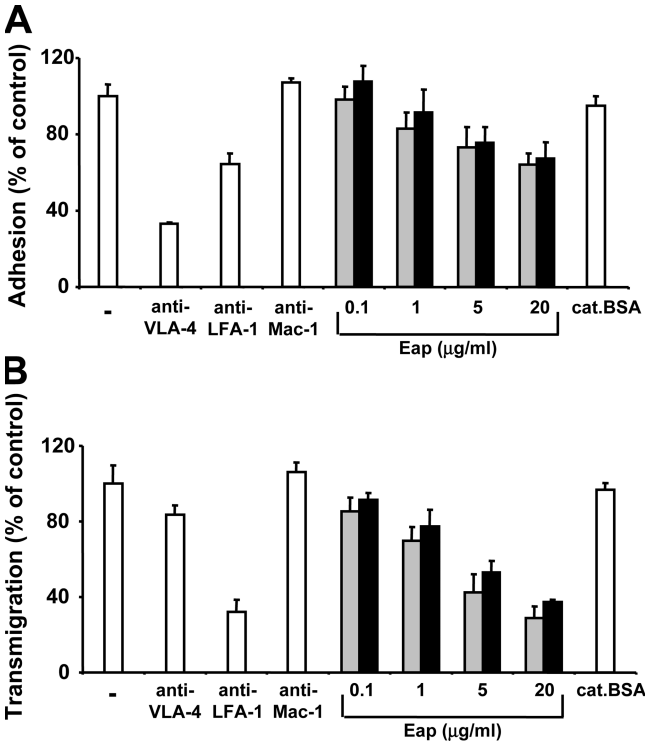

Figure 2. Eap inhibits T cell–endothelial cell interactions. (A) The adhesion of T cells to TNF-α prestimulated HUVEC (10 ng/ml, 16 h) is shown in the absence or presence of blocking mAb against VLA-4, blocking mAb against LFA-1, blocking mAb against Mac-1 (each at 20 μg/ml) (white bars), increasing concentrations of purified Eap (gray bars), recombinant Eap (black bars) or cationic BSA (20 μg/ml; white bars). (B) SDF-1α–stimulated transendothelial migration of T cells is shown in the absence (white bars) or presence of blocking mAb against VLA-4, blocking mAb against LFA-1, blocking mAb against Mac-1 (each at 20 μg/ml) (white bars), increasing concentrations of purified Eap (gray bars), recombinant Eap (black bars), or cationic BSA (20 μg/ml; white bars). Cell adhesion and cell transmigration is expressed relative to control (in the absence of competitor). Data are mean ± SD ($n = 3$) of a typical experiment; similar results were obtained in three separate experiments.

Inhibition of T cell recruitment and delayed type hypersensitivity (DTH) responses in vivo by Eap

To test whether Eap affects T cell–mediated immune responses in vivo, the ability of Eap to interfere with T cell recruitment and cellular immunity was assessed in a DTH model. DTH responses are mediated by infiltrating T cells in response to formerly encountered antigens, resulting in a specific inflammation at the site of local challenge. Mice immunized with oxazolone at day 0 and challenged locally on the right ear on day 5 developed a significant DTH response as measured by ear swelling at day 6 (Fig. 4). Mice treated systemically with either purified or recombinant Eap on day 5 (3 h before local challenge) had a significantly reduced DTH

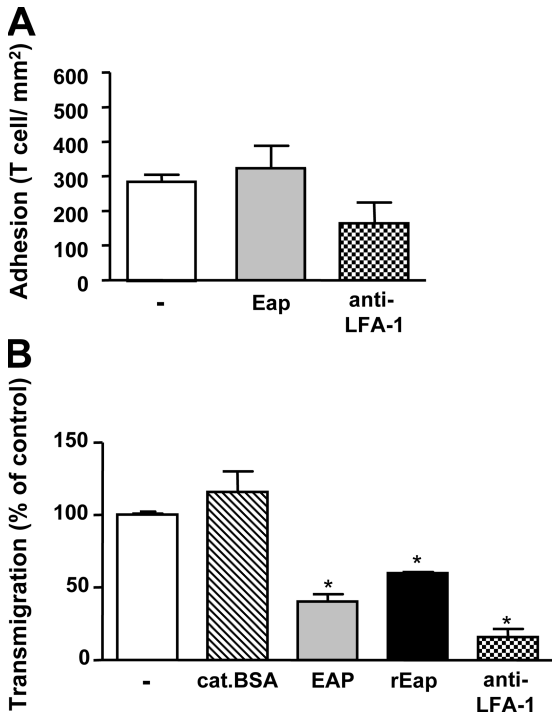

Figure 3. Effect of Eap on T cell–endothelial cell interactions under physiologic flow conditions. T cells were drawn across TNF-α–stimulated endothelial monolayers (25 ng/ml, 4 h) under laminar shear flow conditions (0.76 dynes/mm²). (A) The adhesion of T cells was studied without (white bar) or with purified Eap (gray bar) or anti–LFA-1 mAb (dotted bar) (each 20 μg/ml). (B) The transmigration of T cells was studied without (white bar) or with cationic BSA (diagonally striped bar), purified Eap (gray bar), recombinant Eap (black bar), or anti–LFA-1 mAb (dotted bar) (each 20 μg/ml). T cell adhesion (A) and transmigration relative to control (B) were determined as described in Materials and methods. Data are mean ± SEM, $n = 3$ separate experiments. *, $P < 0.05$.

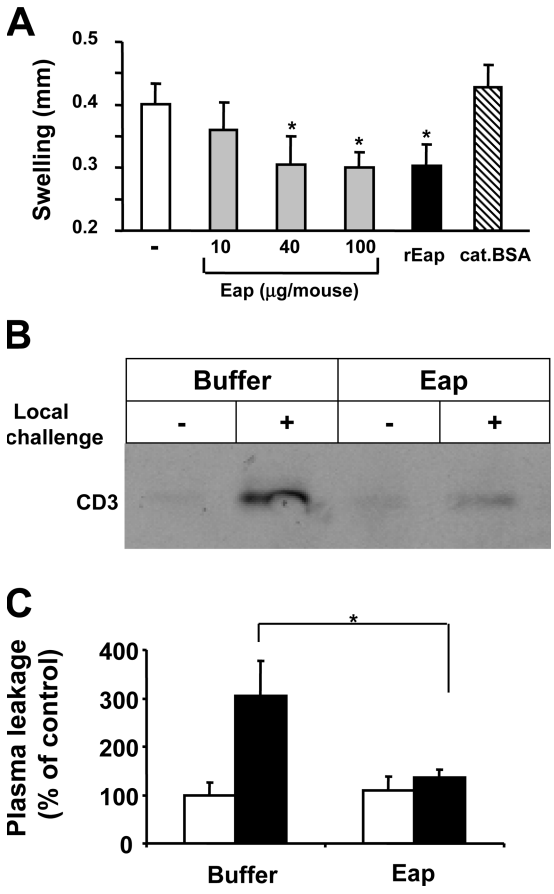

Figure 4. Inhibition of DTH response by Eap. (A) Mice were immunized with OXA (day 0) and at day 5 mice were challenged with local application of OXA on the ear. 2 h before local challenge, mice were treated without (white bar) or with increasing concentrations of purified Eap (gray bars), recombinant Eap (50 μg, black bar), or cationic BSA (100 μg, diagonally striped bar) administered intraperitoneally ($n = 5$ mice/group). Ear thickness was measured after 24 h. The difference in the ear thickness in mm is shown. Data are mean ± SD ($n = 7$). (B) The detection of infiltrated T cells is shown by detection of CD3 in Western blot. Ear tissues from DTH-induced mice that were treated with buffer or Eap were homogenized and the whole tissue lysates were subjected to Western blot to detect the amount of CD3. A typical Western blot for CD3 from the ears of buffer- or Eap-treated mice without (−) or with (+) local challenge using OXA is shown. (C) The vascular leakage (as assessed by influx of Evan's blue) of nonchallenged (white bars) or OXA challenged (black bars) ears is shown in mice pretreated with buffer ($n = 5$) or with Eap ($n = 5$). Ear tissue was removed, dried, and formamide was added to the dried ear tissue to extract Evan's blue; the optical density was registered at 590 nm, as a measure for the content of leaked Evan's blue. Plasma leakage is shown as percent of control (nonchallenged ear of buffer-treated mice) and data are mean ± SD ($n = 5$). *, $P < 0.03$.

response as compared with vehicle-treated but immunized control mice (Fig. 4 A). The effect of Eap was dose dependent and a significant decrease in ear thickness was observed with 40 and 100 μg of purified Eap/mouse ($P < 0.017$ and $P < 0.025$, respectively) (Fig. 4 A).

We examined whether Eap reduced DTH by blocking the local T cell infiltration into the challenged ear. Swollen ear tissues were extracted and homogenized, and equal amounts of tissue lysates were subjected to Western blot analysis for the detection of CD3. As shown in Fig. 4 B, Eap inhibited the recruitment of T cells as indicated by the significant decrease in detection of CD3 as compared with vehicle-treated mice. A major component of the DTH response leading to the ear swelling and the local edema is the increased vascular permeability that also promotes the increased transmigration and recruitment of lymphocytes. We therefore investigated whether Eap treatment reduced the plasma leakage into the inflamed ear by comparing the amounts of Evan's blue dye extracted from the ears of the mice treated with Eap or vehicle. The nonchallenged contralateral ears were used as control to determine the baseline of Evan's blue leakage. Eap treatment significantly reduced Evan's blue leakage by 50–60% compared with the vehicle-treated control (Fig. 4 C). Furthermore, Eap largely prevented TNF-α–induced increased permeability of an endothelial monolayer, as well as the TNF-α–induced morphological changes in the interendothelial junctions (unpublished data).

Prevention of EAE by Eap

Our data up to this point indicate that Eap inhibits T cell recruitment in vitro and in vivo. We therefore tested whether Eap could be used as a therapy in the EAE model. EAE is mediated by autoreactive T cells infiltrating the CNS. EAE was induced as described in Materials and methods and the average onset of the clinical symptoms defining the disease occurred on day 12 after immunization of C57BL/6 mice with myelin oligodendrocyte glycoprotein (MOG) peptides. To determine whether Eap prevents the development of EAE, we treated the immunized mice on days 11, 14, and 17 with purified or recombinant Eap. We tested 10, 25, and 50 μg concentrations of Eap administered on days 11, 14, and 17. Only a subtle reduction of EAE was achieved with 10 μg Eap; however, this reduction was not significant (difference in mean cumulative disease score, $P = 0.4$). In mice that received 25 μg of Eap, we observed an amelioration of EAE from day 18 (i.e., 1 d after completing the treatment on day 17), which remained obvious during the whole course of the experiment (difference in mean cumulative disease score, $P = 0.002$). More strikingly, mice that received 50 μg Eap only marginally developed EAE, with the mean clinical score not exceeding 1 at any time. The prevention of EAE development by 50 μg Eap was maintained throughout the study period (difference in mean cumulative disease score, $P < 0.001$) (Fig. 5 A). In addition, EAE was ameliorated by 50 μg of recombinant Eap (difference in mean cumulative disease score, $P < 0.001$) (Fig. 5 B). In contrast, cationic BSA did not affect the course of EAE, thus excluding a nonspecific effect of the cationic charge of Eap (Fig. 5 B).

However, in a clinical setting of MS, therapeutic intervention is started after the onset of the disease. Hence, the efficacy of Eap treatment for EAE was tested under such conditions. Strikingly, intervention with Eap after the onset of EAE on days 15, 17, and 19 (after initial immunization by MOG peptide) resulted in a prompt clinical recovery from EAE, which was significant even 2 d after the first Eap administration (day 17, $P < 0.032$). Interestingly, the recovery from EAE was sustained until the end of the study (day 33, $P < 0.008$) (Fig. 5 C). Overall, the mean cumulative disease score of Eap-treated mice was significantly lower than that of vehicle-treated mice ($P < 0.001$). In addition, consistent with our data and with the dramatic inhibitory effect on the clinical EAE symptoms by Eap, we found that mononuclear cell infiltrates were strongly reduced or almost absent in the brains of Eap-treated mice compared with the vehicle-treated mice that presented with perivascular and parenchymal inflammatory cell infiltrates (Fig. 6). Furthermore, the T cell recruitment to the brain was inhibited by Eap as indicated by the significant decrease in staining for CD3 in the brains of Eap-treated mice as compared with the brains of vehicle-treated mice (Fig. 6). Collectively, Eap prevented the development of EAE, as well as reverted the disease after its onset as a result of the propensity of the protein to block the infiltration of inflammatory T cells into the brain.

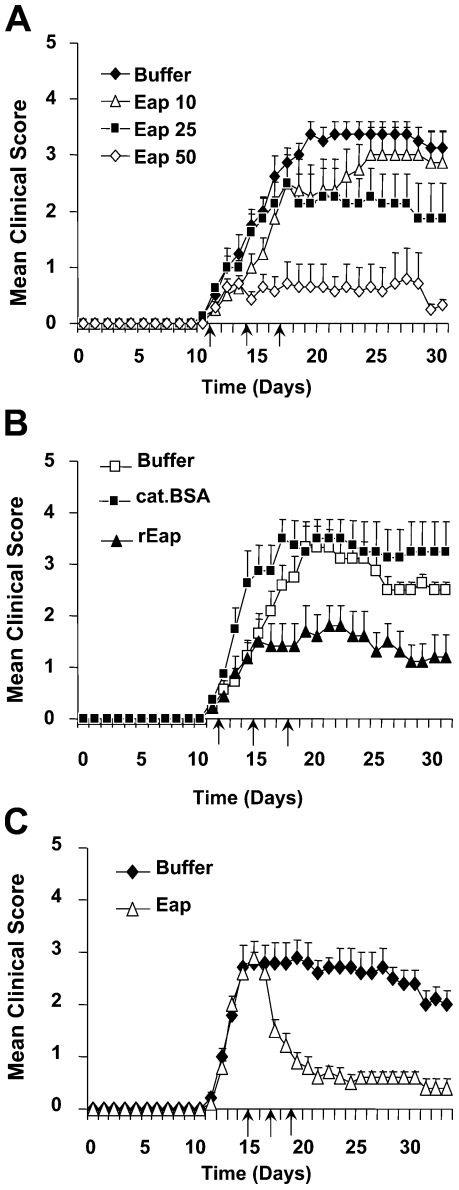

Figure 5. Inhibition of EAE by Eap. MOG-mediated EAE response in mice receiving different treatments. (A) Mice were treated with buffer (closed diamonds) or increasing concentrations of purified Eap (10 μg; open triangles; 25 μg; closed squares; 50 μg, open diamonds) that were administered on days 11, 14, and 17 (arrows) ($n = 5$–8 mice/group). (B) Mice were treated with buffer (open squares), recombinant Eap (50 μg, closed triangles), or cationic BSA (50 μg, closed squares) that were administered on days 11, 14, and 17 (arrows) ($n = 5$ mice/group). (C) Purified Eap (50 μg, open triangles) was administered on days 15, 17, and 19 (arrows) (i.e., after the onset of EAE; $n = 5$ mice/group). Data are represented as the mean clinical score and are mean ± SEM.

DISCUSSION

MS and its mouse counterpart, EAE, is a devastating disease with a very high mortality rate (17, 18). The inflammatory process associated with MS and EAE involves autoreactive T cells and additional cells of the immune system that infiltrate the CNS as well as the breakdown of the BBB (19). These

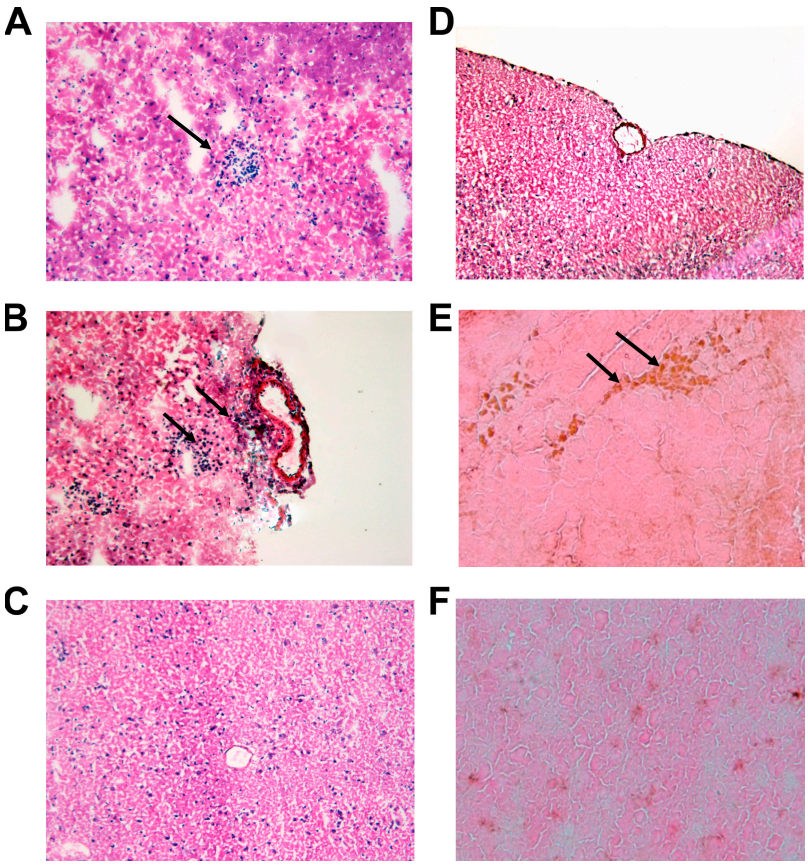

Figure 6. Eap inhibits the infiltration of the CNS by inflammatory cells during EAE. Histology (hematoxylin and eosin staining; A–D) and immunohistology (E–F) from brain sections of EAE mice. Typical photomicrographs indicating parenchymal (A) or perivascular (B) inflammatory cell infiltration in the CNS of buffer-treated mice during EAE. The arrows indicate the inflammatory cell infiltrates. No parenchymal or perivascular cell infiltration was noted in Eap-treated mice (C and D). Massive T cell infiltrates were noted in the brains of buffer-treated mice as indicated by the CD3 staining (E), whereas CD3-positive cells were hardly present in the brains of Eap-treated mice (F).

events are coordinated by chemokines and cytokines as well as by adhesion molecules expressed by both the immune cells and the activated endothelium, especially involving the VLA-4–VCAM-1 and the LFA-1–ICAM-1 adhesion systems (20). The need of therapies for MS and EAE particularly targeting adhesion molecules to limit T cell homing is growing, especially after the withdrawal of natalizumab, an antibody against VLA-4 that demonstrated encouraging efficacy in ameliorating clinical relapses of MS (9). The design of such therapies has to be specific in targeting to increase efficacy and reduce the risk of potential side effects. Our present work clearly demonstrates that the potent antiinflammatory *S. aureus*–derived Eap may provide the basis for the development of a promising novel therapeutic approach for the treatment of MS.

The following three features concur with a potent inhibitory effect of Eap on T cell recruitment in vitro and in vivo to effectively interfere with the development and progression of EAE. First, in vitro, purified and recombinant Eap specifically targeted LFA-1–ICAM-1– but not VLA-4–VCAM-1–mediated T cell recruitment. Consistent with a stronger involvement of the latter adhesion pathway in T cell adhesion to endothelial cells and of the former with T cell transendothelial migration (7, 8, 14, 16), we observed a strong inhibitory effect of Eap on T cell transendothelial migration as opposed to a weak inhibitory effect on T cell adhesion to endothelial cells under physiologic flow conditions. Second, in vivo, we found that purified and recombinant Eap blocked T cell recruitment and the consequent clinical responses to exogenous antigen in the DTH model. Our data in this model are consistent with a previous report by Lee et al. (21); although in that report, Eap was administered during both the induction and effector phases, whereas in our study administration of Eap during the effector phase was sufficient to block DTH. Moreover, we demonstrate here that Eap reduced the vascular permeability that occurred during the inflammatory response in DTH. Third, Eap prevented the development of EAE and markedly reduced infiltration of immune cells to the CNS. Strikingly, intervention with Eap after the onset of EAE clinical symptoms effectively suppressed EAE and reversed the clinical symptoms almost completely. Interestingly, the inhibitory effect of Eap on EAE persisted even after Eap was discontinued, whereas "rebound"

elevated EAE symptoms were observed after stopping administration of the antibody against VLA-4 (22). The inhibitory effects of Eap could not be attributed to its cationic charge because cationic BSA was not effective in any of the experimental systems used in our study.

Our finding that Eap blocks the LFA-1–ICAM-1 system as a therapeutic modality for EAE are in line with the delay of EAE onset by anti–LFA-1 or anti–ICAM-1 antibodies (5, 6). In contrast, ICAM-1–deficient mice exhibited enhanced EAE symptoms (23). A similar controversy has also been reported for PECAM-1–deficient mice, which were shown to have an earlier onset of EAE (24). Thus, besides differences in the animal strains and the experimental models used that may account for these discrepancies, it is clear that therapeutic studies may not correspond to studies with genetically manipulated mice.

Our data support the conclusion that Eap blocks EAE through interfering with the LFA-1–ICAM-1 adhesion pathway that mediates T cell recruitment most likely as a result of its inhibitory effect on transendothelial migration. Consistent with our findings, Laschinger et al. (8) demonstrated that encephalitogenic T cells use LFA-1 for transendothelial migration but not for adhesion to spinal cord microvessels in vivo. However, during the course of EAE, migration of immune cells to the CNS takes place in two phases (25). In the first phase, newly emigrated T lymphocytes recognize their antigen and trigger the inflammatory response, which leads to initiation of the second phase, during which the inflammation-dependent breakdown of the BBB and the intense secondary infiltration of other inflammatory cells such as macrophages is prominent (26). Activated T cells with a TH1 cytokine profile are central in coordinating these processes (27). This inflammatory response also involves the enhanced expression of adhesion molecules on the endothelial cells closely related to the damage of the BBB (28). As the LFA-1–ICAM-1 adhesion pathway mediates this secondary inflammatory cell recruitment in part, we speculate that Eap interferes with this process and thus accounts for the strong Eap-induced suppression of EAE, even after its onset. However, most studies to date have focused on the adhesive events regulating the infiltration of encephalitogenic T cells, although interfering with this secondary inflammatory response may be a more feasible therapeutic approach in a clinical setting where MS is diagnosed after its onset.

The LFA-1–ICAM-1 interaction is also involved in the antigen presentation process (29, 30, 31). However, our data demonstrate a therapeutic effect of Eap given during the effector phase of EAE and suppressing EAE after its onset. This indicates that, in our study, Eap cannot interfere with the induction phase to inhibit early interactions between immunocompetent cells after exposure to antigen. However, from a (patho-)biologic point of view, it would be intriguing to test whether Eap interferes with antigen presentation. The underlying mechanisms of the immunomodulatory role of Eap (13, 21) will be addressed in detail in future studies. Here, the recent crystallographic analysis of Eap revealed structural similarity to bacterial superantigens (32) that should also be taken into account as well.

The endothelium as an essential architectural component of the BBB plays a crucial role in CNS inflammation. Under physiological conditions, the BBB limits the infiltration of inflammatory cells to the CNS. However, the breakdown of the BBB is a hallmark in the development of EAE and MS, thereby potentiating the inflammatory response (33). Interestingly, we observed that Eap may reduce the TNF-α–induced disruption of endothelial cell contacts and the consequent increase in endothelial permeability in vitro (unpublished data) as well as the barrier dysfunction and plasma leakage in the DTH response in vivo. One could assume that Eap might also have a protective effect on the BBB during the course of EAE that may very well contribute to and account for its excellent therapeutic efficacy.

The advantages of the use of Eap as an antiadhesive treatment of EAE and MS may be manifold. One advantage is that Eap targets endothelial ICAM-1, which is up-regulated on the inflamed endothelium during the EAE (34, 35), whereas antibodies against VLA-4 target a constitutively expressed integrin on the lymphocytes as well as other types of leukocytes. Moreover, Eap seems to interfere specifically with LFA-1–ICAM-1–mediated transendothelial migration, which is downstream of the VLA-4–VCAM-1–mediated initial adhesion of encephalitogenic T cells. Another advantage is that Eap reversed EAE after its onset, whereas application of anti–VLA-4 prevented or ameliorated EAE only if it was initiated before the onset of disease and treatment with anti-VLA-4 during acute disease exacerbated EAE (36). A third advantage is that Eap may exert more beneficial effects as it may interfere with the inflammatory cell recruitment secondary to the infiltration of encephalitogenic T cells and may protect BBB breakdown. Together, our present work clearly demonstrates that Eap may prove a novel and promising therapy for the treatment of MS.

MATERIALS AND METHODS

Mice and cell culture. Female C57BL/6 mice were obtained from The Charles River Wiga and housed in the animal facilities of the University of Heidelberg. Mice were used between 10 and 12 wk of age. All animal studies were approved by the governmental office in Karlsruhe, Germany. HUVECs were cultivated in endothelial cell culture media from PromoCell as described previously (37). In experiments performed under flow conditions, HUVECs were isolated and cultured as described previously (15), and $CD3^+$ T cells were isolated from sodium-citrated anticoagulated whole blood drawn from healthy volunteers as described previously (15). Informed consent for blood donations was provided according to the Declaration of Helsinki and according to the Brigham and Women's Hospital Institutional Review Board–approved protocols for protection of human subjects.

Reagents. The following reagents were provided by the following sources: blocking mAb 6S6 against β1-chain (CD29) (Chemicon); blocking mAb LPM19c against Mac-1 (Acris); and mAb HP2.1 against integrin α4-chain, (Immunotech). Blocking mAb against LFA-1, L15 was provided by Y. van Kooyk (VU University Medical Center, Amsterdam, The Netherlands). Recombinant ICAM-1 and VCAM-1, TNF-α were obtained from R&D Systems. FITC-conjugated mAb to human CD3 for flow cytometry was obtained from BD Biosciences. Rat anti–mouse CD3 (MCA1477)

for Western blot and immunostaining as well as stromal cell–derived factor-1α (SDF1α) were obtained from Serotec. Cationic BSA was purchased from Sigma-Aldrich.

Eap purification. Eap from *S. aureus* strain Newman was purified as described previously with modifications (13). In brief, bacteria were harvested after a 20-h incubation in BHI medium (4 × 500 ml) at 37°C. The resultant 1-M lithium chloride-treated extract was dialyzed against PBS, concentrated, and adsorbed onto SP Sepharose (GE Healthcare) in loading buffer (30 mM phosphate buffer, pH 7.0, 200 mM NaCl) at 4°C overnight. After stepwise elution with increasing NaCl concentrations, the pooled eluted fractions (between 0.6 and 0.8 M NaCl) were dialyzed against 1:4 diluted PBS at 4°C and concentrated using Millipore centricon centrifugal filter devices (MWCO 30 kD; Millipore). The rententate (containing 2 mg/ml Eap) was further purified by cation exchange chromatography on Mono S 10/100 GL tricorn column using an ÄKTA fast performance liquid chromatography system (GE Healthcare), operated with 10 mM Tris/HCl, pH 8.0, and an increasing linear NaCl gradient (0–1 M NaCl). Eap-containing fractions were purified on a Superdex 75 HR 10/30 gel filtration column and equilibrated with TBS at pH 7.4, and Eap-positive fractions were pooled, concentrated by ultrafiltration (1–1.5 mg/ml), sterile filtered, and snap frozen at −80°C until further use. Eap revealed a single protein at 64 kD upon SDS-PAGE and was devoid of detectable endotoxin.

Expression and purification of recombinant Eap. A designer gene fragment encoding the entire predicted mature form of Eap from *S. aureus* strain Mu50 was PCR amplified from genomic DNA using oligonucleotides to append SalI and NotI sites at its 5′ and 3′ ends, respectively. The amplified product was digested with the appropriate restriction endonucleases, subcloned into the corresponding sites of the prokaryotic expression vector pT7HMT (38), and sequenced in its entirety to confirm the integrity of the Eap coding region.

After sequencing, the Eap expression plasmid was transformed into *Escherichia coli* strain BL21 (DE3) and the resulting strain was cultured, induced, harvested, and lysed under denaturing conditions according to published protocols (38). After centrifugation (25,000 *g* for 30 min at 20°C), the clarified extract from 1 L of original culture was applied to a 7.5-ml column of chelating sepharose fast flow (GE Healthcare) that had been previously charged with Ni_2SO_4 and equilibrated at 20°C in denaturing wash buffer (20 mM NaH_2PO_4, pH 6.0, 500 mM NaCl, 20 mM imidazole, 8 M urea). Once the entire sample had entered the column, contaminating proteins were washed away with 75 ml of denaturing wash buffer and the specifically bound proteins were eluted with 15 ml of a similar buffer containing 200 mM imidazole. The denatured, purified Eap was refolded by rapid dilution into 150 ml of native binding buffer as described previously (20 mM Tris, pH 8.0, 0.5 M NaCl; reference 38). Then, the refolded recombinant Eap was concentrated by application to an identical chelating column equilibrated at 4°C in native binding buffer. Once the entire sample had entered, the column was washed with 75 ml of native binding buffer and the bound proteins were eluted with 15 ml of a similar buffer containing 500 mM imidazole.

After initial purification, the vector-encoded affinity tag was proteolytically removed from Eap by digestion with recombinant Tobacco Etch Virus protease as described previously (38). Once digestion was complete (as judged by SDS-PAGE), the entire proteolysis reaction was buffer exchanged into 20 mM ethanolamine, pH 9.0, using a HiPrep 26/10 Desalting column (GE Healthcare). Untagged Eap was separated from the residual protease and affinity tagged by cation-exchange chromatography on a 6-ml Resource S column (GE Healthcare), where the bound proteins were resolved by gradient elution to 1 M NaCl in ethanolamine buffer over 60 ml. The final purity of Eap was estimated at >95% (as judged by SDS-PAGE) with a yield of ∼15 mg Eap per liter of original culture. Purified Eap was buffer exchanged into double-deionized water, lyophilized, and stored at −80°C before reconstitution. The final Eap protein contained the additional residues Gly-Ser-Thr at its amino terminus as a result of the subcloning and proteolysis procedures.

Preparation of PBT cells. Human PBMCs were isolated from heparin anticoagulated blood from healthy donors by Histopaque-1107 (Sigma-Aldrich) density gradient centrifugation. PBT cells were separated and purified from PBMCs using Pan-T cells isolation kit obtained from Miltenyi Biotec. The purity of T cells was shown to be >97% measured as CD3 positive using flow cytometry.

PBT adhesion to endothelial cells and transendothelial migration under static conditions. Adhesion of PBT cells to immobilized ICAM-1 or VCAM-1 or to cultured monolayers of HUVECs prestimulated for 16 h with TNF-α was tested as described previously (37, 39). In brief, plates were coated with ICAM-1 or VCAM-1 (10 μg/ml each) in PBS for 16 h at 4°C. HUVECs were grown to confluency onto 96-well plates and were stimulated for 16 h with TNF-α, and medium was changed before the addition of PBT cells. Fluorescently labeled PBT cells (10^5/well) were washed twice and added to the ICAM-1– or VCAM-1–coated wells or to HUVECs and were incubated at 37°C for 60 min in the absence or presence of inhibitors. After washing, adhesion of PBT cells was quantified using a fluorescence microplate reader (Bio-Tek).

Transendothelial migration was performed as described previously (39). In brief, transmigration assays were performed using 6.5-mm transwell filters with a 5-μm pore size (Corning Costar). After inserts were coated with gelatine (Sigma-Aldrich), HUVECs were seeded onto transwell filters 2 d before the assay and grown without medium in the lower compartment for 48 h in a humidified atmosphere (37°C, 5% CO_2). At the beginning of the transmigration assay, 600 μl migration assay medium (serum-free RPMI 1640 in the absence or presence of SDF1α) was added to the lower compartment of the transwell system. PBT cells (3×10^5 in 100 μl) were added to the upper compartment on top of the endothelial monolayer. After incubation for 4 h at 37°C the number of transmigrated cells in the lower compartment was estimated with a cell-counter (CASY-Counter; Schärfe-System). The inserts were washed twice in PBS and fixed with methanol, stained with crystal violet, and mounted on glass slides to confirm the confluence of the endothelial monolayer of the filters after the assay.

PBT adhesion and transmigration assays under physiological flow conditions. Glass coverslips (25-mm dia, Carolina Biological Supply) were coated with 2.5 μg/ml of ICAM-1 or VCAM-1 and 2 μg/ml of stromal cell-derived factor-1α (CXCL12, SDF-1α)(Peprotech). SDF-1α pretreatment has been shown to promote T cell adhesion to the integrin ligands (14). Where indicated, coverslips were treated with purified Eap, recombinant Eap, or cationic BSA or T cells were treated with function-blocking anti–LFA-1 mAb (TS1/22; American Type Culture Collection). PBT cell interactions with immobilized ICAM-1 or VCAM-1 were examined under conditions of fluid shear stress in a parallel plate flow chamber as described previously (40). In brief, PBT cells were drawn through the chamber at decreasing flow rates corresponding to an estimated shear stress of 1 dyne/cm^2, 0.76 dynes/cm^2, and 0.5 dynes/cm^2. T cell accumulation was determined after the initial minute of each flow rate by counting the number of cells in four different fields. T cell interactions with substrates were recorded using a 20× phase contrast objective, videomicroscopy, and VideoLab software. For PBT cell adhesion to HUVECs and transendothelial migration, confluent HUVECs grown on 25-mm dia glass coverslips coated with 5 μg/ml fibronectin (Sigma-Aldrich) were stimulated with TNF-α (25 ng/ml) for 4 h and inserted into the flow chamber. Where indicated, HUVECs were treated with 20 μg/ml Eap. Lymphocytes (10^6/ml) suspended in flow buffer (Dulbecco phosphate-buffered saline/0.1% human serum albumin) were drawn across HUVECs at 0.76 dyne/cm^2 for 3 min, followed by buffer alone for 10 min. HUVEC monolayers were incubated with 50 ng/ml of SDF-1α during 15 min before assay to promote T-lymphocyte TEM (14, 41). Live-cell imaging of leukocyte TEM was performed using a digital imaging system coupled to a Nikon TE2000 inverted microscope as described previously (15). Sequential images of differential interference contrast (DIC) were taken every 15 s for 10 min in a representative field from 3 min after the start of leukocyte perfusion. The total number of accumulated leukocytes

was determined by counting total adherent and transmigrated cells in five fields. The percentage of TEM = total transmigrated leukocytes/(total adhered + transmigrated leukocytes) × 100. $P \leq 0.05$ was considered statistically significant using the paired Student's *t* test or one-way analysis of variance for multiple groups.

DTH responses. Mice were sensitized by topical application of a 2% oxazolone (4-ethoxymethylene-2-phenyl-2-oxazoline-5-one; OXA; Sigma-Aldrich) solution in acetone/olive oil (4:1 vol/vol) onto the shaved abdomen (50 μl) (day 0). On day 5, the right ears were challenged by topical application of 10 μl of a 1% oxazolone solution on both sides of the ear, whereas the left ears were treated with vehicle alone. 3 h before local challenge, mice were treated with different concentrations of purified or recombinant Eap administered intraperitoneally. Ear thickness was measured after 24 h (day 6) using a spring-loaded micrometer (Mitutoyo). Measurement of ear thickness was performed by a researcher who was not aware of the treatment groups. The ear swelling was calculated by the difference in the thickness between right ears (OXA treated) and left ears (vehicle treated).

For the detection and quantification of CD3, ear tissues from DTH-induced mice were homogenized and equal amounts of tissue lysates were subjected to SDS-PAGE. Western blot analysis with antibody MCA1477 was performed to detect CD3.

Measurement of vascular leakage. Vascular leakage was measured as described previously (42). DTH-induced mice were injected intracardially with 100 μl Evan's blue dye (30 mg/kg) 24 h after OXA challenge. After 10 min, mice were killed and ear tissues were removed, dried at 55°C overnight, and weighed. Evan's blue was extracted from the dried ear tissue by incubation in formamide for 48 h and absorbance was measured at 590 nm in a microplate reader (BIO-TEK).

Induction of EAE. MOG p35–55, MEVGWYRSPFSRVVHLYRNGK, was purchased from TebuBio. Mice were immunized with 200 μg MOG peptide emulsified in Freund's incomplete adjuvant (Sigma-Aldrich) together with 5 mg/ml *Mycobacterium tuberculosis* H37RA (Difco). A total of 100 μl emulsion was subcutaneously injected into four sites on the flanks of mice near the tail. At days 0 and 2 after the initial peptide injections, animals received additional injections of 400 ng pertussis toxin (Difco) intraperitoneally. Different concentrations of purified or recombinant Eap or cationic BSA in 400 μl PBS (or the same volume of vehicle) were administered intraperitoneally at the times indicated in the figure legends.

Mice were scored daily for clinical assessment of disease based on the following criteria: 0, normal; 1, limp tail or hind limb weakness; 2, limp tail and hind limb weakness; 3, partial hind limb paralysis; 4, complete hind limb paralysis; and 5, moribund or dead. Food and water was made accessible to immobile animals, and moribund animals with a score of 5 were killed. A score of 5 was not included in the calculation of daily mean clinical score. Clinical scoring was performed by a researcher who was not aware of the treatment groups.

For the histological and immunohistological analysis of the CNS in the EAE model, mice brains were snap frozen in liquid nitrogen and embedded in OCT compound. Specimens were cut into 3-μm cross sections. To evaluate CNS infiltrates, sections were stained with hematoxylin and eosin or anti-CD3 mAb followed by eosin counterstaining.

Statistical analysis. For the analysis of the effect of Eap on the DTH response, one-way analysis of variance with Holm-Sidak post-hoc analysis (α value was set to 0.05) was performed. For the analysis of the effect of Eap on EAE, the Mann-Whitney U test was used for comparison between groups. Statistical analysis was performed by using SigmaStat3.1 (Systat Software Inc.).

We acknowledge U. Schubert and A. Sobke for technical assistance and Dr. G.M. Shearer for critically reading this manuscript.

This work was supported in part by the Intramural Research Program of the National Institutes of Health (NIH), National Cancer Institute (to T. Chavakis); by grants from the Deutsche Forschungsgemeinschaft: nos. SFB405 (to T. Chavakis) and SPP1130 (to T. Chavakis, M. Herrmann, K.T. Preissner); by NIH grant nos. HL56985, HL36028, and HL53393 (to F.W. Luscinskas); by a Fullbright/Spanish Ministry of Education and Science grant (to P. Alcaide), and by grant no. 2509 from the University of Missouri Research Board (to B.V. Geisbrecht).

The authors have no conflicting financial interests.

Submitted: 19 August 2005
Accepted: 10 March 2006

REFERENCES

1. 't Hart, B.A., and S. Amor. 2003. The use of animal models to investigate the pathogenesis of neuroinflammatory disorders of the central nervous system. *Curr. Opin. Neurol.* 16:375–383.
2. Springer, T.A. 1994. Traffic signals for lymphocyte recirculation and leukocyte emigration: the multistep paradigm. *Cell.* 76:301–314.
3. Yednock, T.A., C. Cannon, L.C. Fritz, F. Sanchez-Madrid, L. Steinman, and N. Karin. 1992. Prevention of experimental autoimmune encephalomyelitis by antibodies against α4 β1 integrin. *Nature.* 356:63–66.
4. Baron, J.L., J.A. Madri, N.H. Ruddle, G. Hashim, and C.A. Janeway Jr. 1993. Surface expression of α4 integrin by CD4 T cells is required for their entry into brain parenchyma. *J. Exp. Med.* 177:57–68.
5. Gordon, E.J., K.J. Myers, J.P. Dougherty, H. Rosen, and Y. Ron. 1995. Both anti-CD11a (LFA-1) and anti-CD11b (MAC-1) therapy delay the onset and diminish the severity of experimental autoimmune encephalomyelitis. *J. Neuroimmunol.* 62:153–160.
6. Archelos, J.J., S. Jung, M. Maurer, M. Schmied, H. Lassmann, T. Tamatani, M. Miyasaka, K.V. Toyka, and H.P. Hartung. 1993. Inhibition of experimental autoimmune encephalomyelitis by an antibody to the intercellular adhesion molecule ICAM-1. *Ann. Neurol.* 34:145–154.
7. Oppenheimer-Marks, N., L.S. Davis, D.T. Bogue, J. Ramberg, and P.E. Lipsky. 1991. Differential utilization of ICAM-1 and VCAM-1 during the adhesion and transendothelial migration of human T lymphocytes. *J. Immunol.* 147:2913–2921.
8. Laschinger, M., P. Vajkoczy, and B. Engelhardt. 2002. Encephalitogenic T cells use LFA-1 for transendothelial migration but not during capture and initial adhesion strengthening in healthy spinal cord microvessels in vivo. *Eur. J. Immunol.* 32:3598–3606.
9. Steinman, L. 2005. Blocking adhesion molecules as therapy for multiple sclerosis: natalizumab. *Nat. Rev. Drug Discov.* 4:510–518.
10. Cannella, B., A.H. Cross, and C.S. Raine. 1993. Anti-adhesion molecule therapy in experimental autoimmune encephalomyelitis. *J. Neuroimmunol.* 46:43–55.
11. Harraghy, N., M. Hussain, A. Haggar, T. Chavakis, B. Sinha, M. Herrmann, and J.I. Flock. 2003. The adhesive and immunomodulating properties of the multifunctional *Staphylococcus aureus* protein Eap. *Microbiology.* 149:2701–2707.
12. Chavakis, T., K. Wiechmann, K.T. Preissner, and M. Herrmann. 2005. *Staphylococcus aureus* interactions with the endothelium: the role of bacterial "secretable expanded repertoire adhesive molecules" (SERAM) in disturbing host defense systems. *Thromb. Haemost.* 94:278–285.
13. Chavakis, T., M. Hussain, S.M. Kanse, G. Peters, R.G. Bretzel, J.I. Flock, M. Herrmann, and K.T. Preissner. 2002. *Staphylococcus aureus* extracellular adherence protein serves as anti-inflammatory factor by inhibiting the recruitment of host leukocytes. *Nat. Med.* 8:687–693.
14. Cinamon, G., V. Shinder, and R. Alon. 2001. Shear forces promote lymphocyte migration across vascular endothelium bearing apical chemokines. *Nat. Immunol.* 2:515–522.
15. Rao, R.M., T.V. Betz, D.J. Lamont, M.B. Kim, S.K. Shaw, R.M. Froio, F. Baleux, F. Arenzana-Seisdedos, R. Alon, and F.W. Luscinskas. 2004. Elastase release by transmigrating neutrophils deactivates endothelial-bound SDF-1α and attenuates subsequent T lymphocyte transendothelial migration. *J. Exp. Med.* 200:713–724.
16. Luscinskas, F.W., H. Ding, and A.H. Lichtman. 1995. P-selectin and vascular cell adhesion molecule 1 mediate rolling and arrest, respectively, of $CD4^+$ T lymphocytes on tumor necrosis factor α-activated vascular endothelium under flow. *J. Exp. Med.* 181:1179–1186.

17. Lublin, F.D. 2005. Clinical features and diagnosis of multiple sclerosis. *Neurol. Clin.* 23:1–15 (v.).
18. Flachenecker, P., and P. Rieckmann. 2004. Health outcomes in multiple sclerosis. *Curr. Opin. Neurol.* 17:257–261.
19. Sospedra, M., and R. Martin. 2005. Immunology of multiple sclerosis. *Annu. Rev. Immunol.* 23:683–747.
20. Kennedy, K.J., and W.J. Karpus. 1999. Role of chemokines in the regulation of Th1/Th2 and autoimmune encephalomyelitis. *J. Clin. Immunol.* 19:273–279.
21. Lee, L.Y., Y.J. Miyamoto, B.W. McIntyre, M. Hook, K.W. McCrea, D. McDevitt, and E.L. Brown. 2002. The *Staphylococcus aureus* Map protein is an immunomodulator that interferes with T cell-mediated responses. *J. Clin. Invest.* 110:1461–1471.
22. Brocke, S., C. Piercy, L. Steinman, I.L. Weissman, and T. Veromaa. 1999. Antibodies to CD44 and integrin α4, but not L-selectin, prevent central nervous system inflammation and experimental encephalomyelitis by blocking secondary leukocyte recruitment. *Proc. Natl. Acad. Sci. USA.* 96:6896–6901.
23. Samoilova, E.B., J.L. Horton, and Y. Chen. 1998. Experimental autoimmune encephalomyelitis in intercellular adhesion molecule-1-deficient mice. *Cell. Immunol.* 190:83–89.
24. Graesser, D., A. Solowiej, M. Bruckner, E. Osterweil, A. Juedes, S. Davis, N.H. Ruddle, B. Engelhardt, and J.A. Madri. 2002. Altered vascular permeability and early onset of experimental autoimmune encephalomyelitis in PECAM-1-deficient mice. *J. Clin. Invest.* 109:383–392.
25. Chavarria, A., and J. Alcocer-Varela. 2004. Is damage in central nervous system due to inflammation? *Autoimmun. Rev.* 3:251–260.
26. Hickey, W.F. 1999. Leukocyte traffic in the central nervous system: the participants and their roles. *Semin. Immunol.* 11:125–137.
27. Krakowski, M.L., and T. Owens. 1997. The central nervous system environment controls effector $CD4^+$ T cell cytokine profile in experimental allergic encephalomyelitis. *Eur. J. Immunol.* 27:2840–2847.
28. Karpus, W.J., and R.M. Ransohoff. 1998. Chemokine regulation of experimental autoimmune encephalomyelitis: temporal and spatial expression patterns govern disease pathogenesis. *J. Immunol.* 161:2667–2671.
29. Jenkins, M.K., and J.G. Johnson. 1993. Molecules involved in T-cell costimulation. *Curr. Opin. Immunol.* 5:361–367.
30. Sharpe, A.H. 1995. Analysis of lymphocyte costimulation in vivo using transgenic and 'knockout' mice. *Curr. Opin. Immunol.* 7:389–395.
31. Lebedeva, T., M.L. Dustin, and Y. Sykulev. 2005. ICAM-1 co-stimulates target cells to facilitate antigen presentation. *Curr. Opin. Immunol.* 17:251–258.
32. Geisbrecht, B.V., B.Y. Hamaoka, B. Perman, A. Zemla, and D.J. Leahy. 2005. The crystal structures of EAP domains from *Staphylococcus aureus* reveal an unexpected homology to bacterial superantigens. *J. Biol. Chem.* 280:17243–17250.
33. Petty, M.A., and E.H. Lo. 2002. Junctional complexes of the blood-brain barrier: permeability changes in neuroinflammation. *Prog. Neurobiol.* 68:311–323.
34. Sharief, M.K., M.A. Noori, M. Ciardi, A. Cirelli, and E.J. Thompson. 1993. Increased levels of circulating ICAM-1 in serum and cerebrospinal fluid of patients with active multiple sclerosis. Correlation with TNF-α and blood-brain barrier damage. *J. Neuroimmunol.* 43:15–21.
35. Lou, J., M. Chofflon, C. Juillard, Y. Donati, N. Mili, C.A. Siegrist, and G.E. Grau. 1997. Brain microvascular endothelial cells and leukocytes derived from patients with multiple sclerosis exhibit increased adhesion capacity. *Neuroreport.* 8:629–633.
36. Theien, B.E., C.L. Vanderlugt, T.N. Eagar, C. Nickerson-Nutter, R. Nazareno, V.K. Kuchroo, and S.D. Miller. 2001. Discordant effects of anti-VLA-4 treatment before and after onset of relapsing experimental autoimmune encephalomyelitis. *J. Clin. Invest.* 107:995–1006.
37. Chavakis, T., A. Bierhaus, N. Al-Fakhri, D. Schneider, S. Witte, T. Linn, M. Nagashima, J. Morser, B. Arnold, K.T. Preissner, and P.P. Nawroth. 2003. The pattern recognition receptor (RAGE) is a counter-receptor for leukocyte integrins: a novel pathway for inflammatory cell recruitment. *J. Exp. Med.* 198:1507–1515.
38. Geisbrecht, B.V., S. Bouyain, and M. Pop. 2006. An optimized system for expression and purification of secreted bacterial proteins. *Protein. Expr. Purif.* 46:23–32.
39. Chavakis, T., T. Keiper, R. Matz-Westphal, K. Hersemeyer, U.J. Sachs, P.P. Nawroth, K.T. Preissner, and S. Santoso. 2004. The junctional adhesion molecule-C promotes neutrophil transendothelial migration in vitro and in vivo. *J. Biol. Chem.* 279:55602–55608.
40. Lim, Y.C., L. Henault, A.J. Wagers, G.S. Kansas, F.W. Luscinskas, and A.H. Lichtman. 1999. Expression of functional selectin ligands on Th cells is differentially regulated by IL-12 and IL-4. *J. Immunol.* 162: 3193–3201.
41. Muller, W.A. 2001. Migration of leukocytes across endothelial junctions: some concepts and controversies. *Microcirculation.* 8:181–193.
42. Kunstfeld, R., S. Hirakawa, Y.K. Hong, V. Schacht, B. Lange-Asschenfeldt, P. Velasco, C. Lin, E. Fiebiger, X. Wei, Y. Wu, et al. 2004. Induction of cutaneous delayed-type hypersensitivity reactions in VEGF-A transgenic mice results in chronic skin inflammation associated with persistent lymphatic hyperplasia. *Blood.* 104:1048–1057.